Microstructure and Mechanical Characteristics of Lanthana-Bearing Nanostructured Ferritic Steels

Somayeh Pasebani & Indrajit Charit

Chemical and Materials Engineering
University of Idaho, Moscow, ID

Collaborators:
Darryl P. Butt, Yaqiao Wu, Jatu Burns, Kerry Allahar
(Boise State University)
James Cole (Idaho National Laboratory)
Lin Shao and Lloyd Price (Texas A&M)

Outline

- ***Introduction***
  - Oxide dispersion strengthened steels
  - Applications of ODS alloys as fuel cladding materials
  - Nanostructured ferritic steels
- ***Objectives***
  - Rare earth oxide dispersion
  - Spark plasma sintering
- ***Experimental***
  - Ball milling
  - Spark plasma sintering
  - Ion (Fe^{+2}) irradiation
  - Characterization
- ***Results and Discussion***
  - Effect of milling time, SPS parameters and alloy composition
  - Microanalysis of oxide particles
  - Irradiation behavior
- ***Conclusions***

Introduction

Oxide Dispersion Strengthened (ODS) Steels

- Excellent high temperature creep strength
- Good radiation damage tolerance
- Pioneering work by Fisher in 1982 (INCO): MA956/ MA957
- ODS steels developed for nuclear fission and fusion applications in the US, Japan and Europe

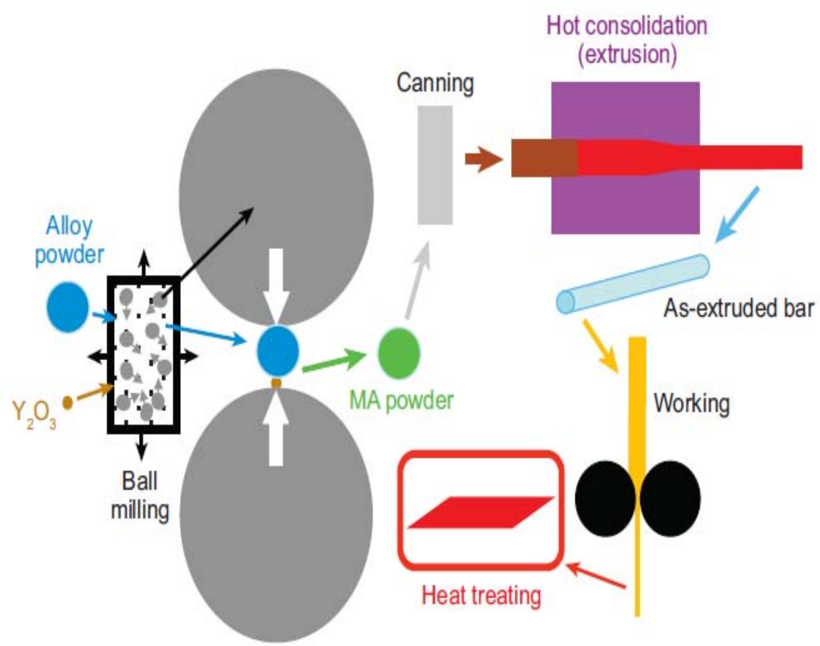

Conventional route for processing ODS alloys

Odette *et al.* (2008)

Oxide Dispersion Strengthened Steels

Alloy	Composition (wt %)									
	Fe	Ni	Cr	Al	Ti	Mo	W	C	Y_2O_3	Other
MA956	bal.	-	20	4.5	0.5	-	-	0.05	0.5	
MA754	1.0	bal.	20	0.3	0.5	-	-	0.05	0.6	
MA758	-	bal.	30	0.3	-	-	0.5	0.05	0.6	
MA760	1.2	bal.	19.5	6.0	-	-	3.4	0.06	1.0	
MA6000	-	bal.	15	4.5	2.5	2.0	4.0	0.05	1.1	2.0Ta; 0.15Zr
MA957	bal.	-	14	-	0.9	0.3	-	0.01	0.25	
PM2000	bal	-	19	5.5	0.5	-	-	0.05	0.5	
PM1000	3.0	bal.	20	0.3	0.5	-	-	0.05	0.6	
PM3030	-	bal.	17	6.0	-	2.0	3.5	0.05	0.9	2.0Ta; 0.15Zr
ODM751	bal.	-	16.5	4.5	0.6	1.5	-	0.05	0.5	

Special Metals Corporation (MA alloys)
Plansee GmbH (PM alloys)
Dour Metal S.A. (now Dour Metal s.r.o.) (ODM751)

ODS Alloys for Nuclear Applications

- Fast reactors: Significant challenges to materials selection (T> 700 ^{o}C and high neutron doses)
- Limitations of some fuel cladding materials:
  - o Zirconium alloys: susceptibility to hydrogen embrittlement, allotropic changes at higher temperatures, poor creep properties
  - o Austenitic stainless steels: swelling
  - o SiC: low thermal conductivity, brittle
  - o Ferritic-Martensitic (F-M) steels: susceptible to radiation hardening, embrittlement and relatively low strength at higher temperatures
- Development of ODS ferritic steels for fast reactors:
  - o Dimensional stability
  - o Thermal and radiation creep resistance
  - o Helium traps (particle/matrix interface) and swelling resistance
  - o Resistance to irradiation hardening/embrittlement

Nanostructured Ferritic Steels (NFSs)

- Strengthened by ultrafine Y-Ti-O-enriched nanofeatures:
  - o Large numbers of stable nanometer-scale precipitates
  - o Fine-scale bubbles
  - o Reduced swelling
  - o Stabilized grain boundaries
  - o High creep strength

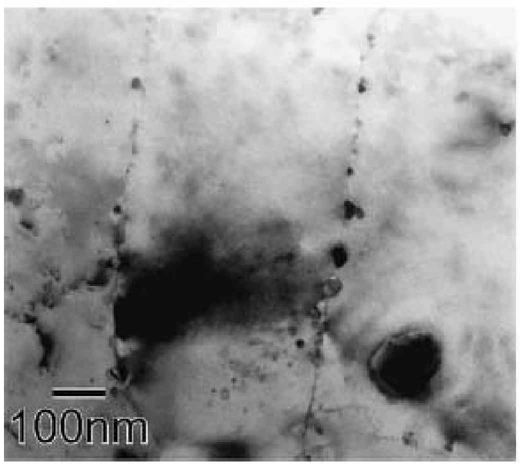

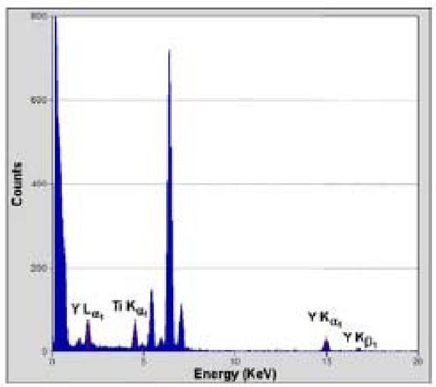

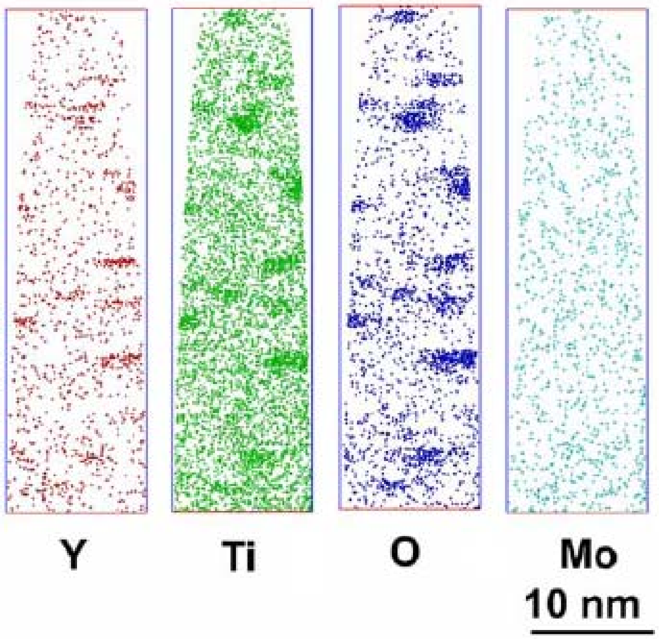

TEM micrograph and APT maps for MA957
Miller *et al.* (2004)

University of Idaho
College of Engineering

Objectives

Rare Earth Oxide Dispersions

- The most commonly used RE oxide: Y_2O_3
- Are there any potential alternative RE oxides?
- Meuller *et al.*, (2000): Dispersion hardening effect of La_2O_3, Y_2O_3 and ZrO_2 in Mo-based ODS alloys demonstrated
  - o Highest UTS and creep-rupture properties with La_2O_3

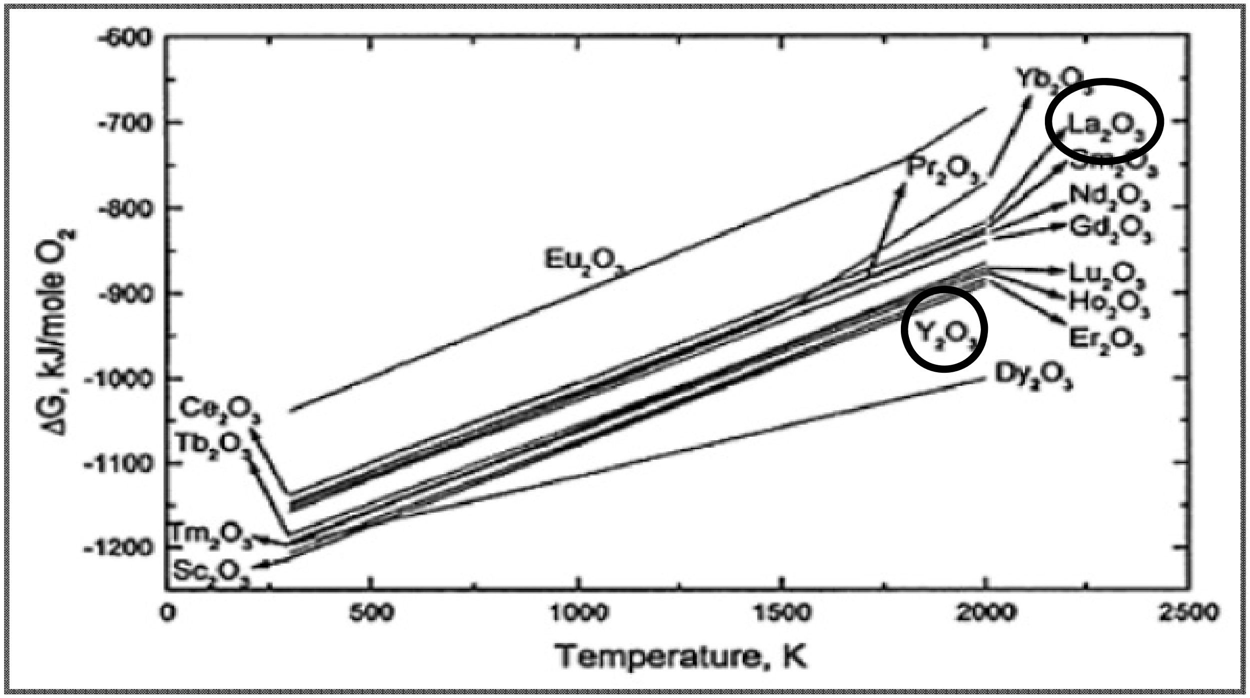

Free energy formation of oxides

Gupta *et al.* (2005)

University *of* Idaho
College *of* Engineering

Spark Plasma Sintering

- Sintering at lower temperatures, shorter dwell times and lower cost
- No texture or anisotropy
- Simultaneous uniaxial pressing and passing of electrical current
- Joule effect
- Local melting, evaporation of oxide layers, surface and volume diffusion enhance the neck formation

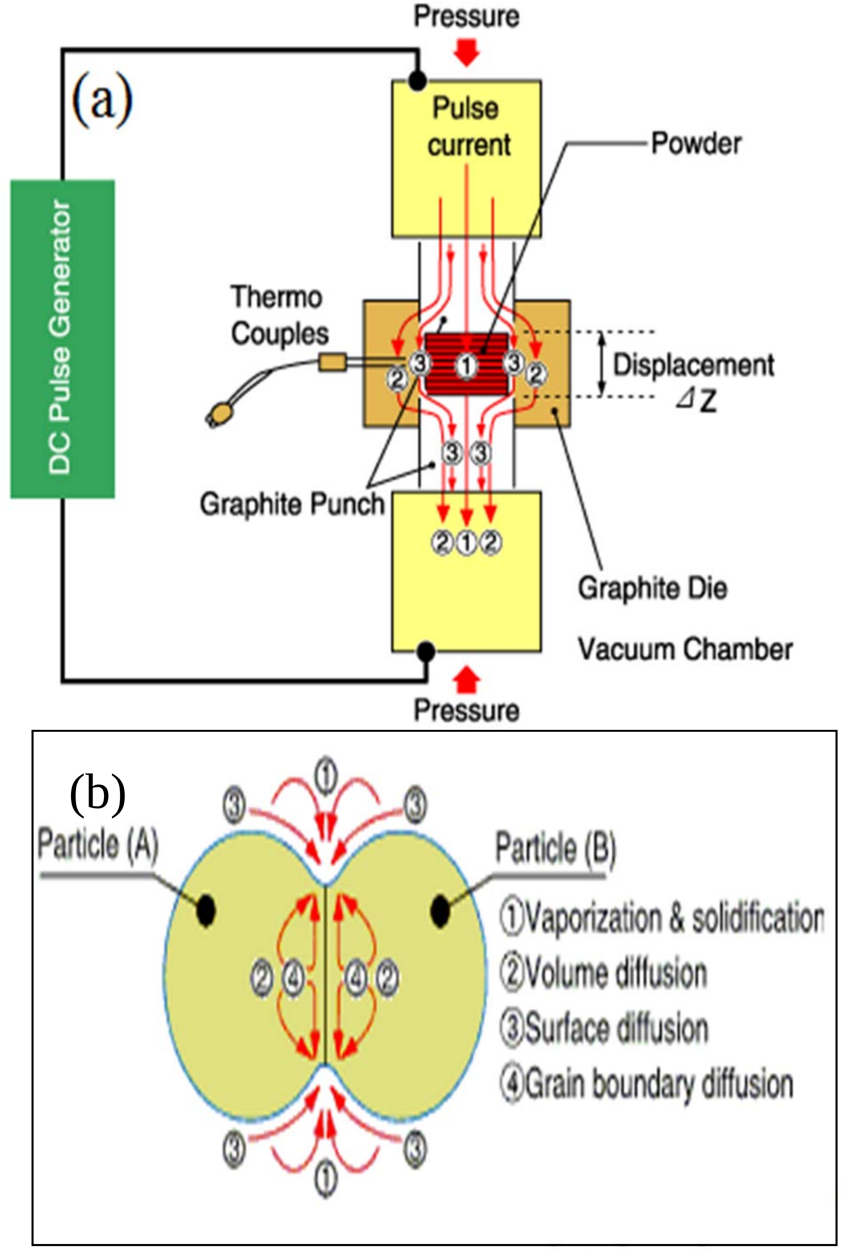

(a) Schematic of SPS and (b) densification mechanisms in SPS

Suárez *et al.*, (2013)

Experimental

Experimental - Ball Milling

- The nominal composition (wt.%):
  - Fe-14Cr-1Ti-0.3Mo-0.5La_2O_3 (14LMT)
  - Fe-14Cr-1Ti-0.3Mo-0.3Y_2O_3 (14YMT)
  - Other compositions
- SPEX 8000M shaker mill:
  - Hardened steel balls (8 mm in diameter)
  - BPR of 10:1
  - Milling time for 0–20 h
- As-milled powder characterization:
  - XRD
  - SEM/EDS
  - Transmission electron microscopy (TEM) and atom probe tomography (APT) studies

Spex mixer/mill

Milling vial and steel balls

University of Idaho
College of Engineering

Experimental - SPS

- Dr. Sinter SPS 515S with maximum current capacity of 1500 A and force of 30 kN
- Consolidating the milled powder via SPS at:
  - Temperature: 850-1050 ^{o}C
  - Time: 0-45 min
  - Pressure: 80 MPa
  - Heating rate: 100 ^{o}C/min
- Under vacuum (7×10^{-3} Torr)
- Tri-Gemini cylindrical graphite die (12.7 mm inner diameter)

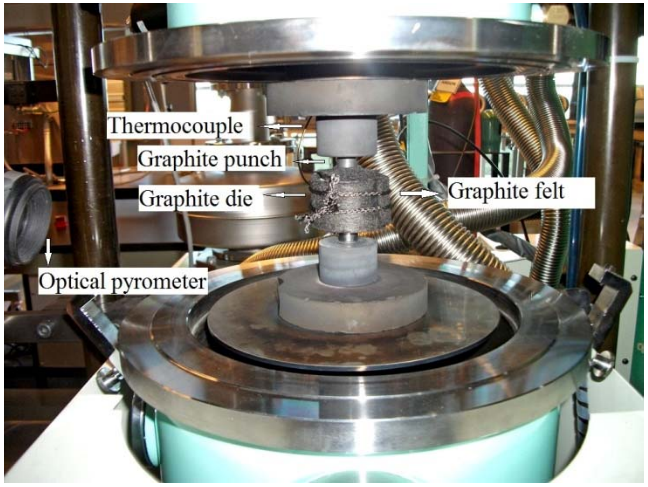

SPS chamber

Sintered samples

University of Idaho
College of Engineering

Experimental - Characterization

- Density measurement
- Mechanical Properties
  - o Vickers microhardness
  - o Compression testing
- Microstructural Characterization
  - o Sample preparation via electrojet-polishing and focused ion beam (FIB)
  - o TEM (JEOL 2010 and FEI Tecnai TF30-FEG STEM)
  - o APT(CAMECA LEAP 4000X HR)

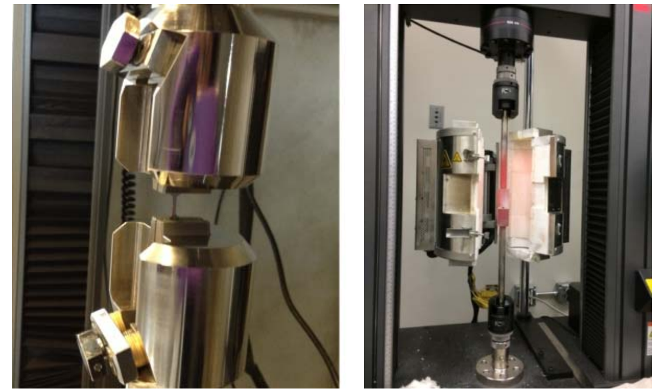

Tensile and compression test set-up

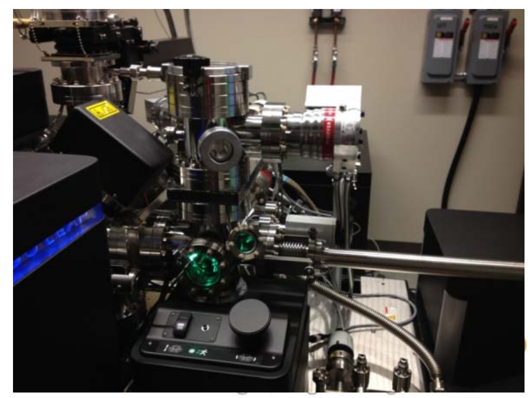

Results & Discussion

Effect of Milling Time on Milled Powder

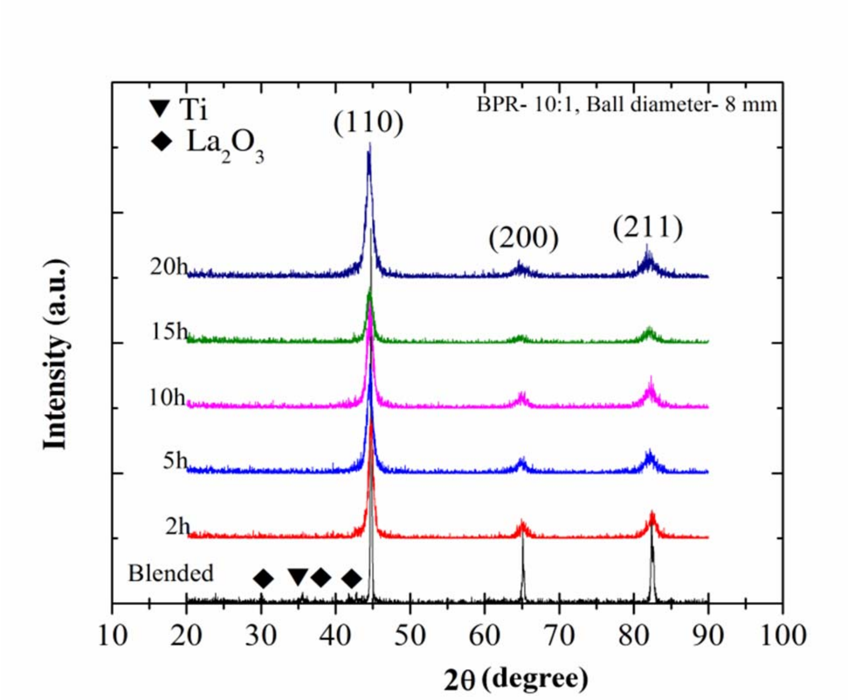

The XRD pattern of 14LMT alloy as a function of milling time

Table 1
Summary of the microstructural characteristics and microhardness of 14LMT powder batches as a function of milling time.

Milling time (h)	Lattice parameter (nm)	Crystallite size (nm)	Lattice strain (%)	Microhardness (HV)	Mean particle size (μm)
0	0.2864 ± 0.0003	388 ± 13	0.10 ± 0.02	330 ± 24	14.1 ± 1.1
2	0.2870 ± 0.0002	150 ± 12	0.50 ± 0.04	591 ± 12	16.6 ± 1.5
5	0.2878 ± 0.0003	76 ± 9	0.66 ± 0.03	851 ± 10	26 ± 2.1
10	0.2881 ± 0.0001	24 ± 8	0.77 ± 0.04	970 ± 20	5.5 ± 1.1
15	0.2881 ± 0.0002	18 ± 5	0.82 ± 0.02	1011 ± 12	7.5 ± 1.2
20	0.2880 ± 0.0002	14 ± 3	0.79 ± 0.02	929 ± 20	24.1 ± 1.8

Pasebani *et al.*, *Acta Materialia* 61 (2013) 5605

Effect of Milling Time on Milled Powder

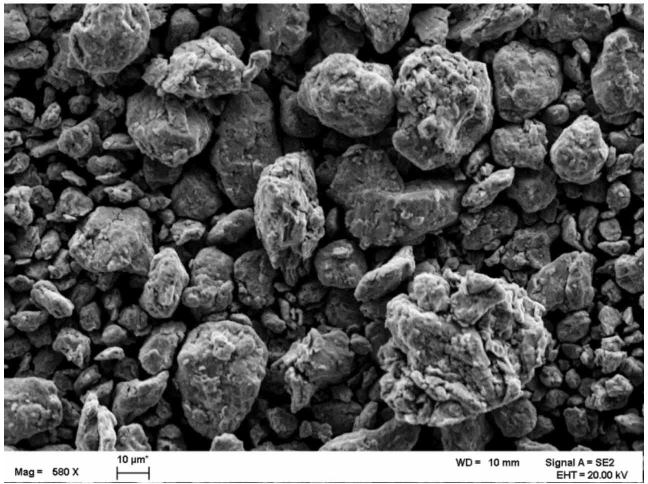

2 h

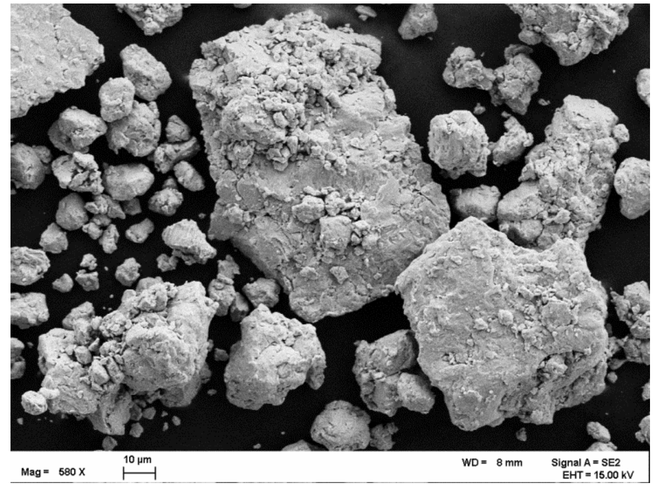

5 h

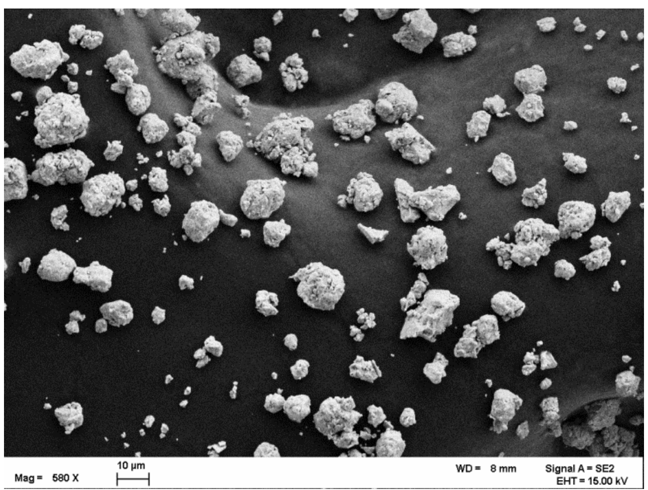

10 h

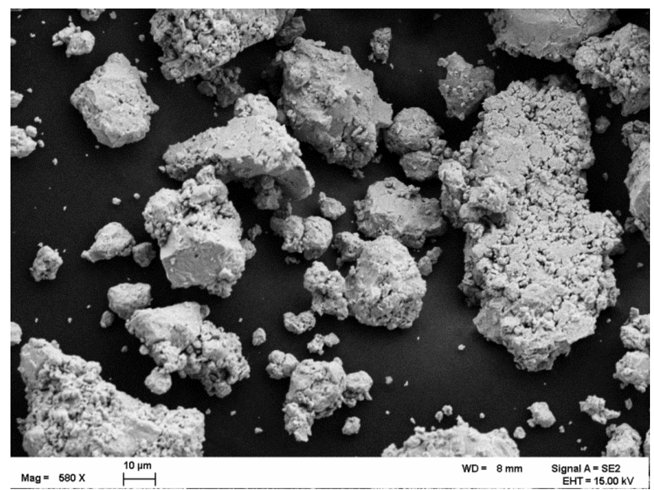

20 h

Pasebani *et al.*, *Acta Materialia* 61 (2013) 5605

Microstructure of Milled Powder

- Heavily deformed microstructure
- Very small crystallite size
- The nanoclusters (NCs) were Cr-, Ti-, La-, O- enriched: the mean radius 0.97 nm
- The nucleation of NCs that occurred during MA will be enhanced during SPS.
- Stable O-vacancy pairs enable nucleation of O-enriched NCs.

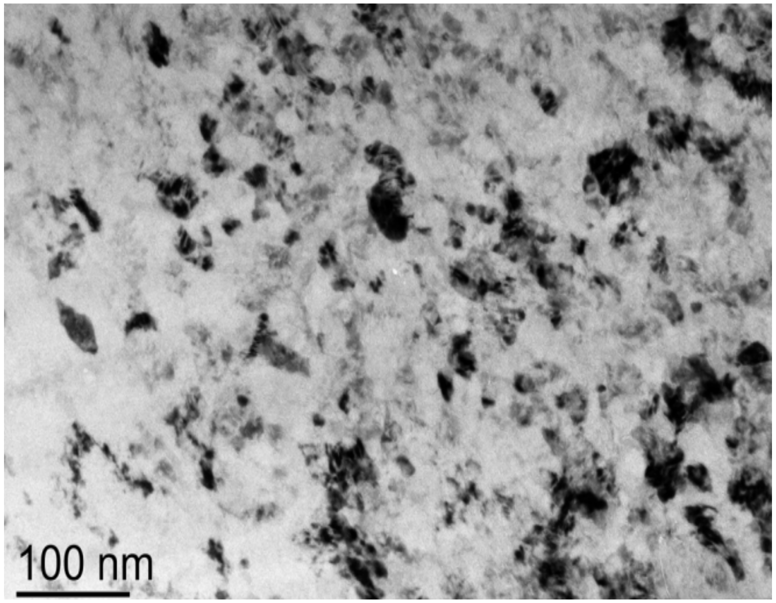

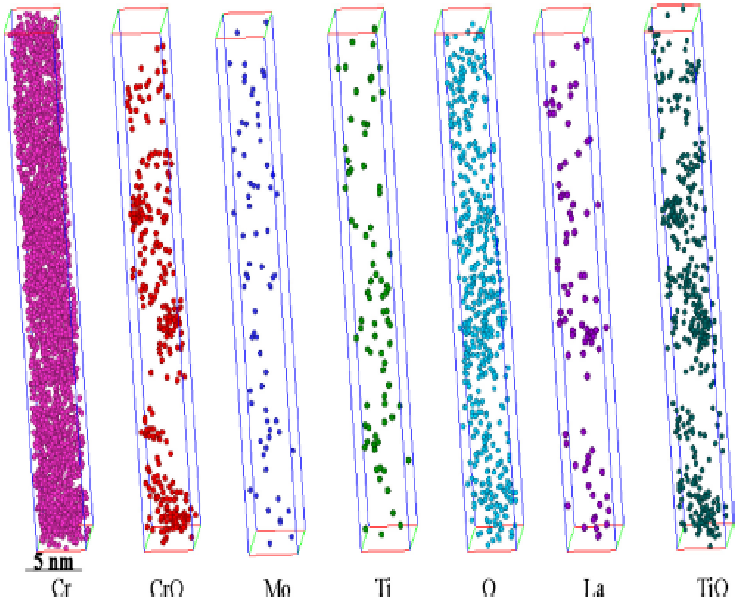

5x5x35 nm^3

Pasebani *et al., J. Nuclear Materials* 434 (2013) 282

Effects of Milling Time on Kinetics

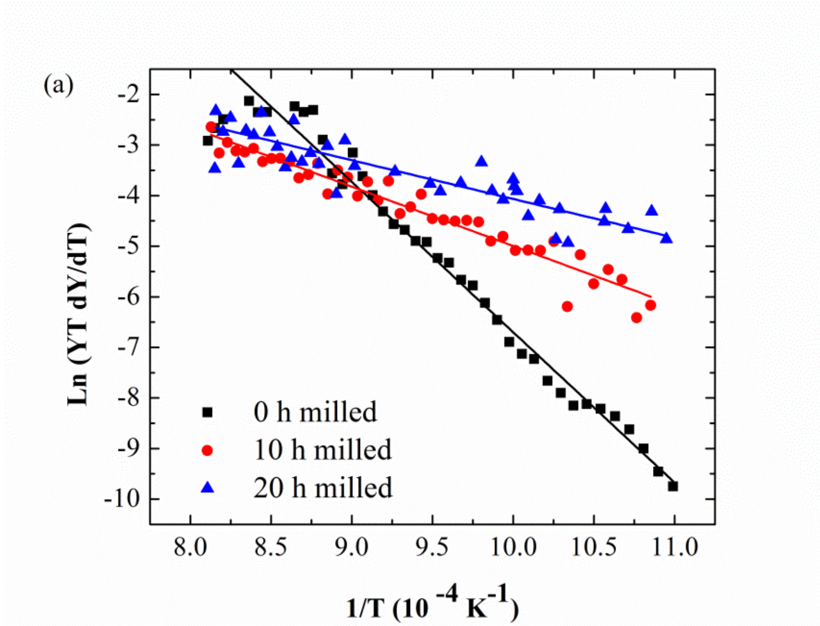

Volume diffusion

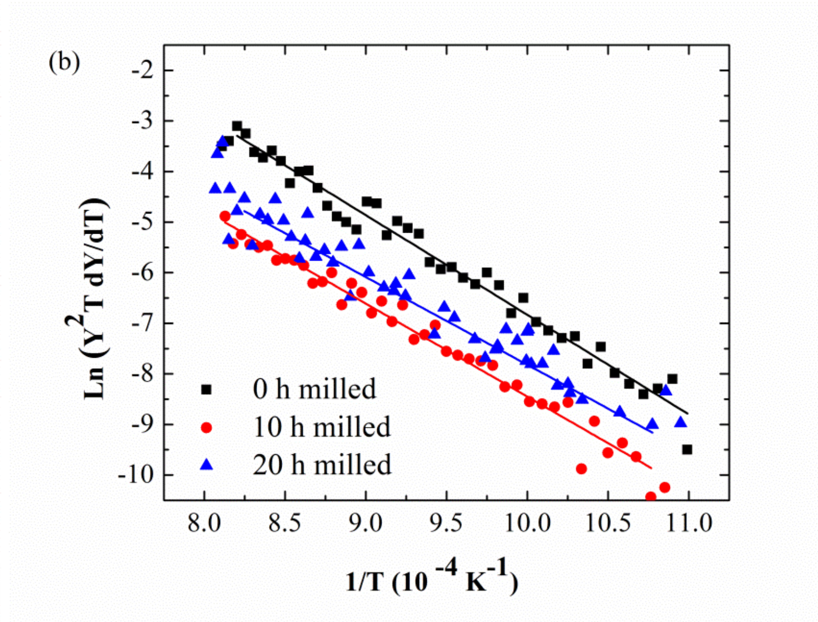

Grain boundary diffusion

$$\ln\left(YT\frac{dY}{dT}\right) = \ln\left(\frac{2.63\gamma\Omega D^0{}_v}{ka^3c}\right) - \frac{Q_v}{RT}$$

$$\ln\left(Y^2T\frac{dY}{dT}\right) = \ln\left(\frac{0.71\gamma b\Omega D^0 b}{ka^4c}\right) - \frac{Q_b}{RT}$$

- Activation energy for volume diffusion:
  - o 247±6, 98±4 and 64±6 kJ/mol (0, 10 and 20 h)
- Activation energy for grain boundary diffusion:
  - o 153±5, 164±4 and 144±15 kJ/mol (0, 10 and 20 h)

Effect of Milling Time on Sintered Microstructure

- Micron sized grains after sintering with no milling
- Nanograins after milling for 5 h and sintering
- A bimodal type of grain structure at longer milling times
- Such bimodal present in HIP or extrusion, too
- No strong texture

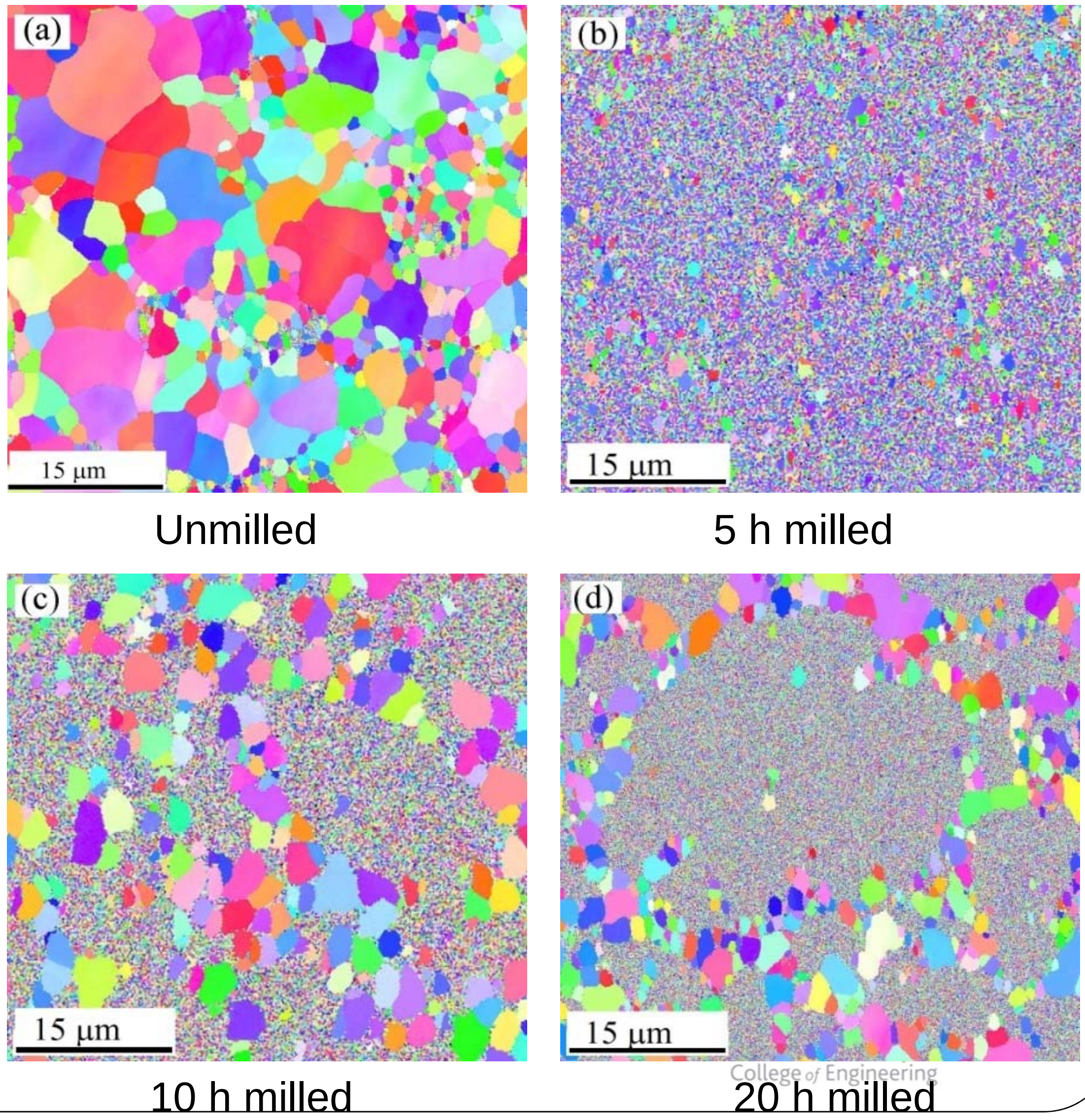

Effects of Milling Time on Microstructure (Contd.)

- No bimodal structure in unmilled/sintered 14LMT sample with average grain size 2.5 μm
- Bimodal grain size after 10 and 20 h
- Nanograins with high dislocation density and smaller particles
- Micron sized grains with low dislocation density and larger particles

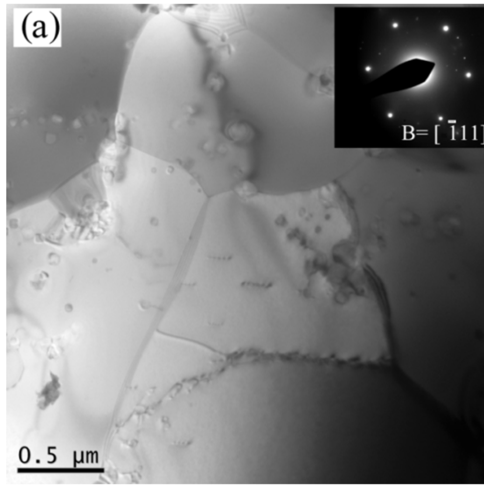

Unmilled

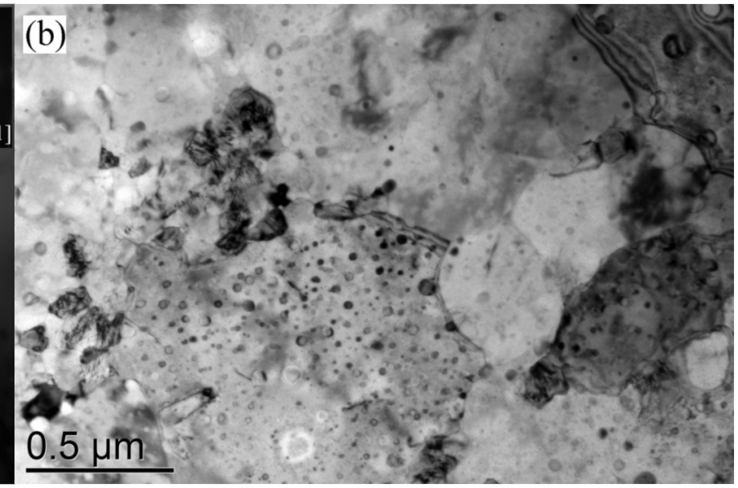

10 h milled

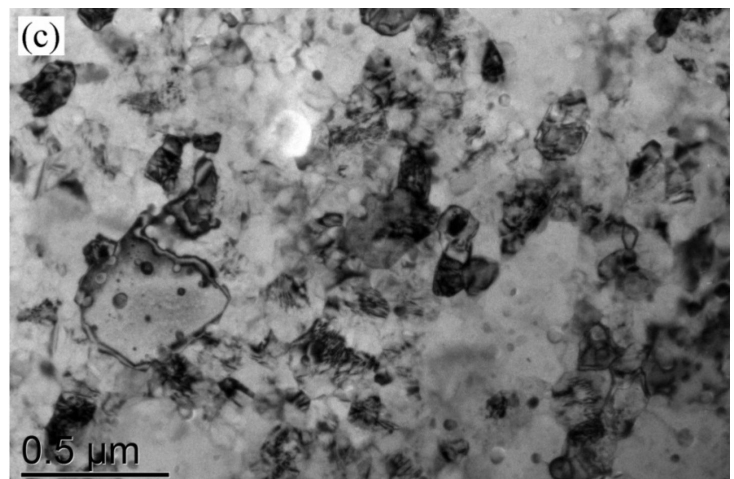

20 h milled

Effect of SPS Parameters on Microstructure

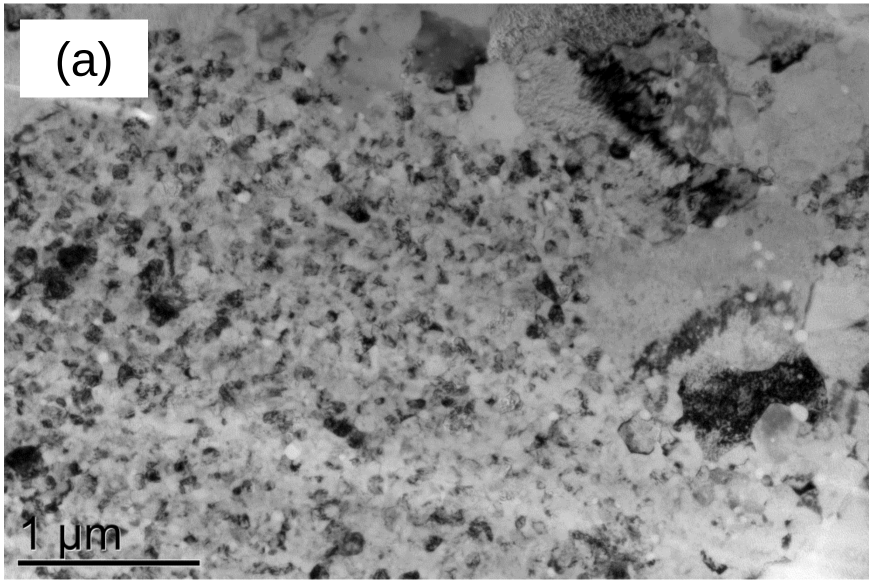

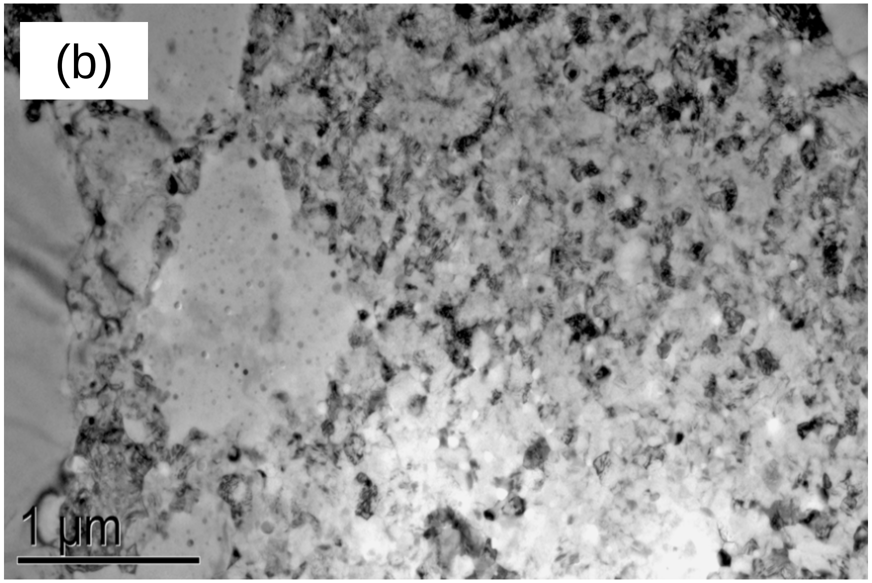

14LMT alloy SPSed at 850 °C for 45 min

14LMT alloy SPSed at 950 °C for 45 min

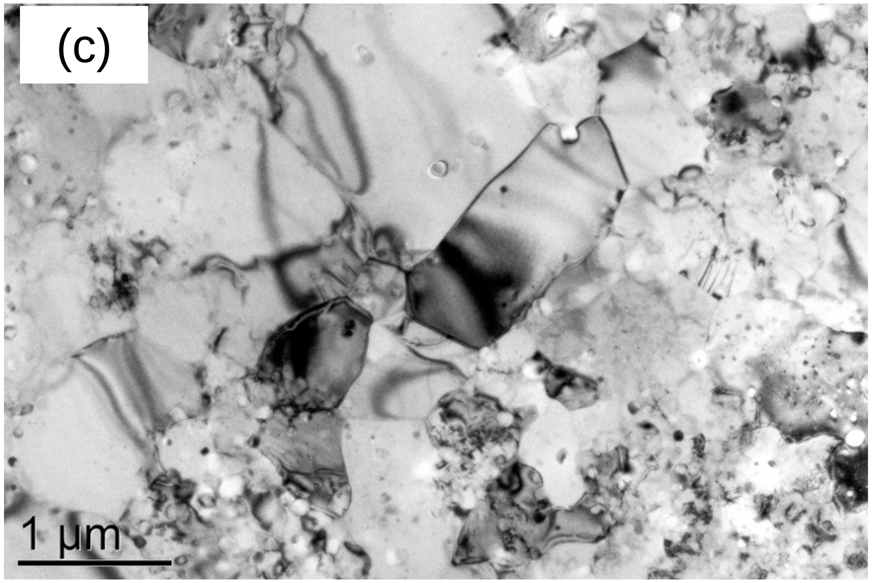

14LMT alloy SPSed at 1050 °C for 45 min

University of Idaho
College of Engineering

Microanalysis of Oxide Particles

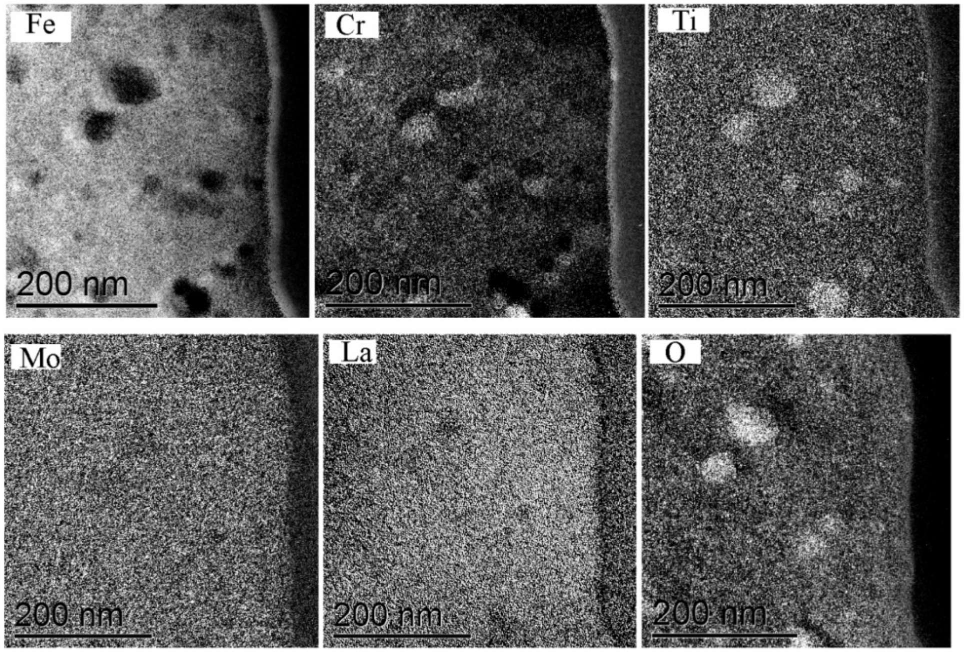

EFTEM elemental maps from raw data showing different elements in 14LMT alloy SPSed at 950 ^{o}C for 45 min

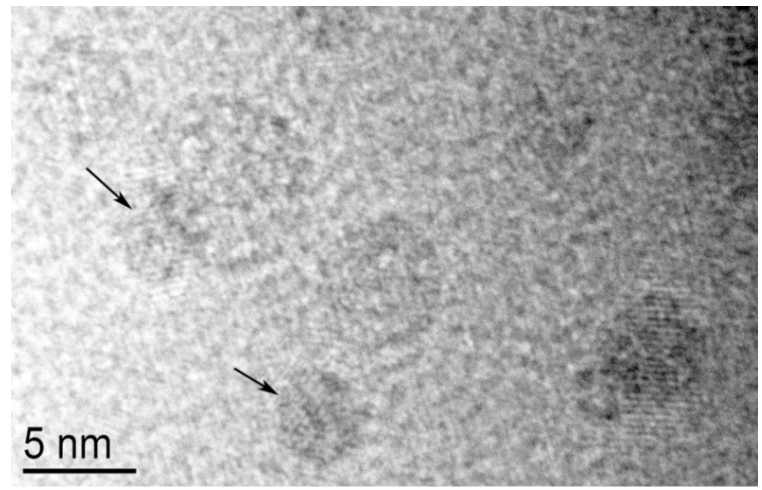

HRTEM micrograph of particle

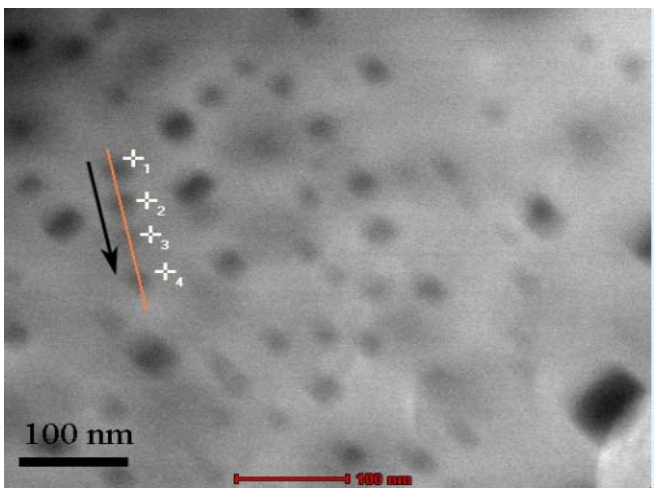

STEM HAADF micrograph of particles

•Ti and La were mostly concentrated in the particles smaller than 10 nm.

University of Idaho
College of Engineering

Microanalysis of Nanoclusters
APT Analysis

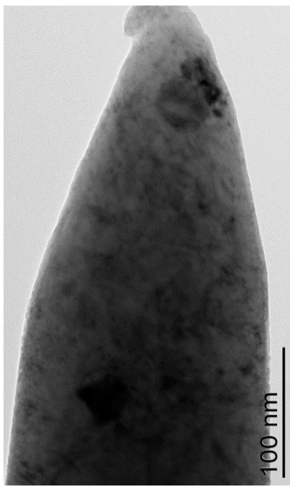

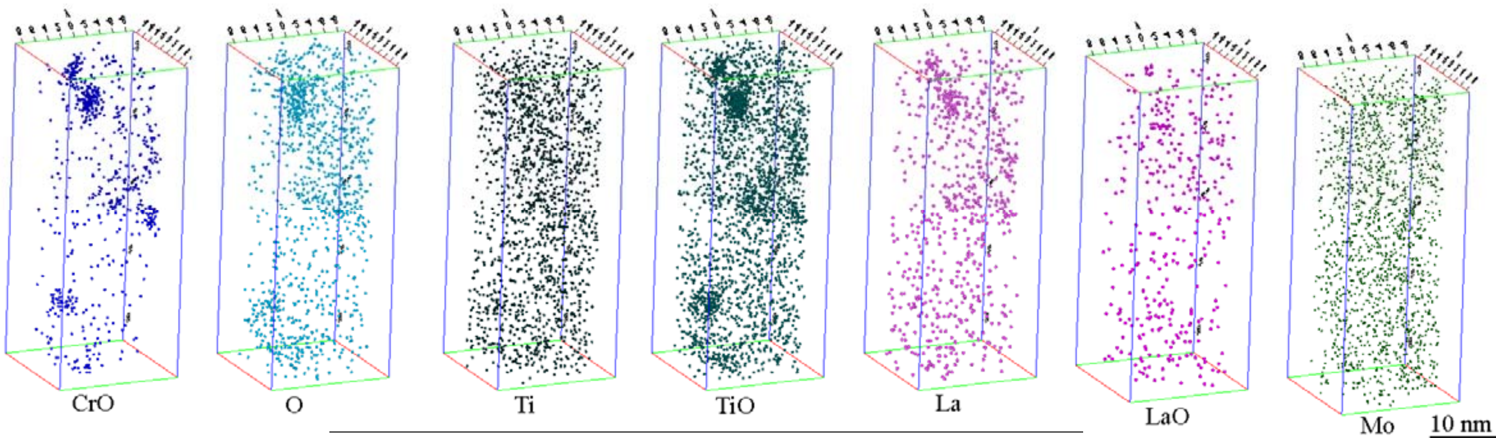

- NCs - no. density 1.2×10^{24} m^{-3} with an average radius of 1.5±0.3 nm

Compositional measurements

Element	Bulk (at.%)	Matrix (at.%)	Cluster (at.%)	Matrix-corrected (at.%)
Cr	13.88±0.5	10.73±0.3	8.9±2.2	31.82±3.2
O	0.39±0.1	0.12±0.06	35.25±3.2	34.2±4.3
Ti	1.09±0.09	0.25±0.1	17.8±2.0	25.5±2.1
C	0.1±0.05	0.10±0.05	0.05±0.04	0.09±0.05
N	0.09±0.04	0.10±0.05	0.04±0.02	0.04±0.05
La	0.14±0.06	0.05±0.04	7.89±0.84	10.31±0.1
Mo	0.17±0.05	0.16±0.05	0.06±0.03	0.04±0.04
Fe	84.14±0.5	88.49±0.3	32.01±6.4	0.0

Effect of SPS Parameters on Mechanical Properties

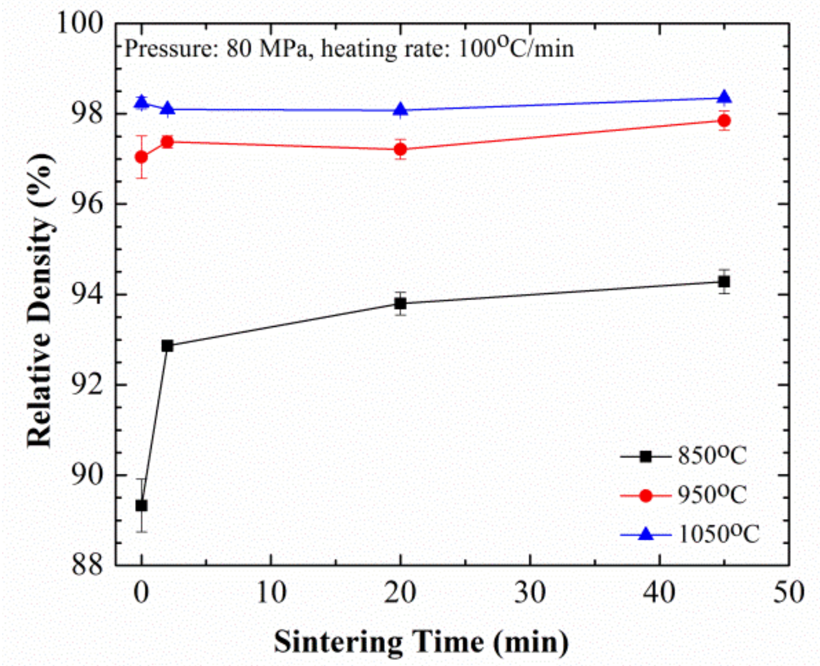

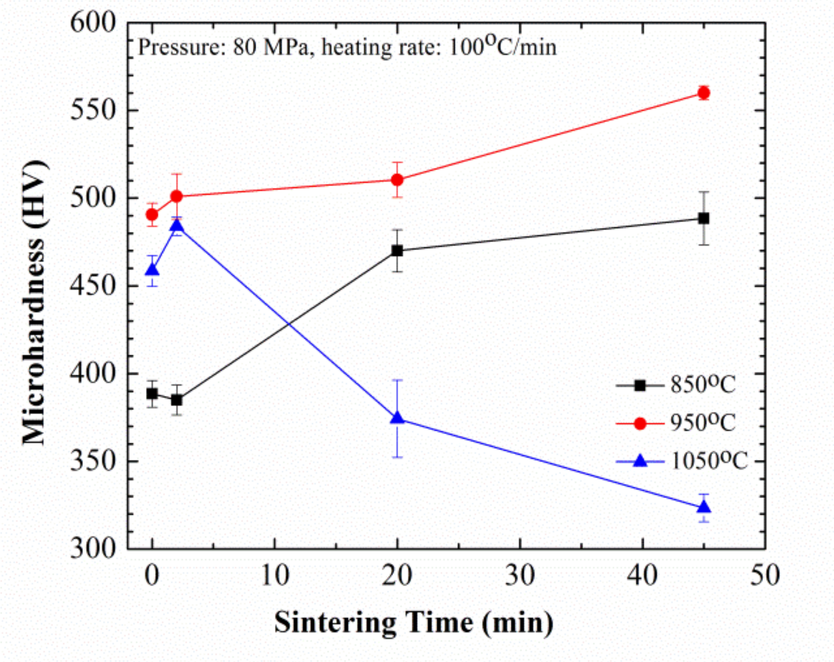

- The relative density values after SPS at 850, 950 and 1050 °C for 45 min were 94.3%, 97.8% and 98.3%, respectively.
- Microhardness: 488, 561 and 324 HV, after SPS at 850, 950 and 1050 °C for 45 min, respectively.

University of Idaho
College of Engineering

Mechanical Properties

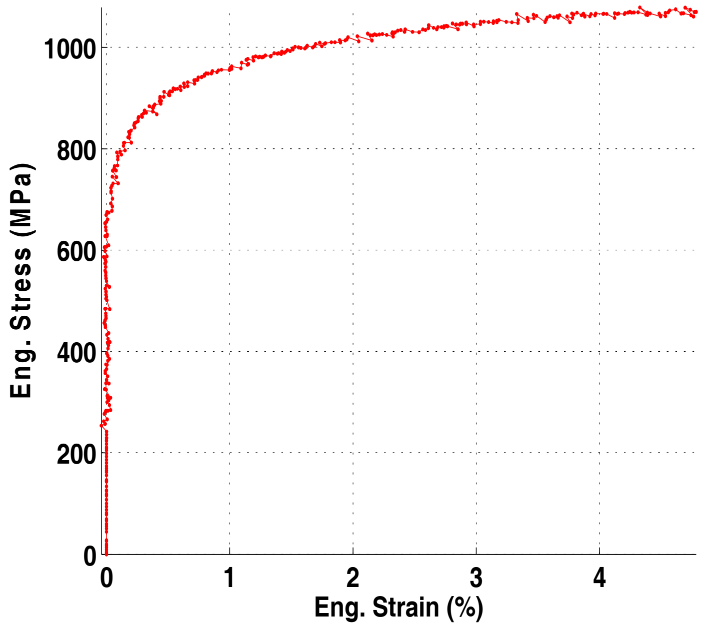

Tensile test at strain rate of 10^{-3} s^{-1}

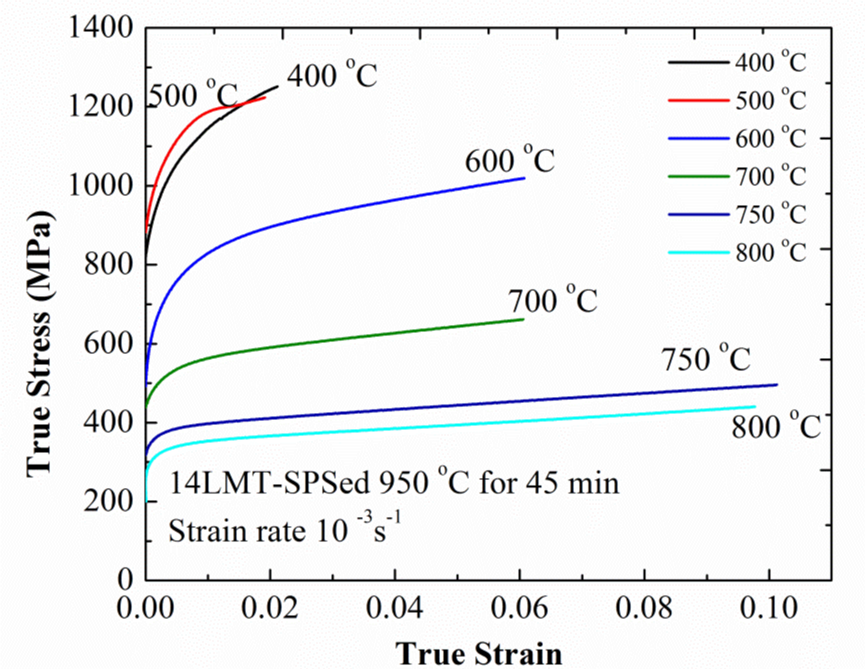

Compression test at strain rate of 10^{-3} s^{-1}

- Tensile test at room temperature: 0.2% YS - 836 MPa
- Strength is retained to a high level even at very high temperatures: Compression yield strength of 326 MPa at 800 °C

University of Idaho
College of Engineering

Effect of Alloy Composition on Microstructure

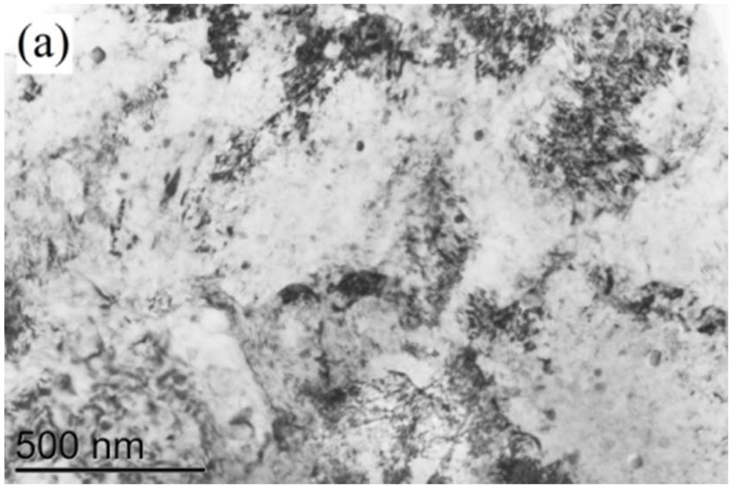

Fe-14Cr

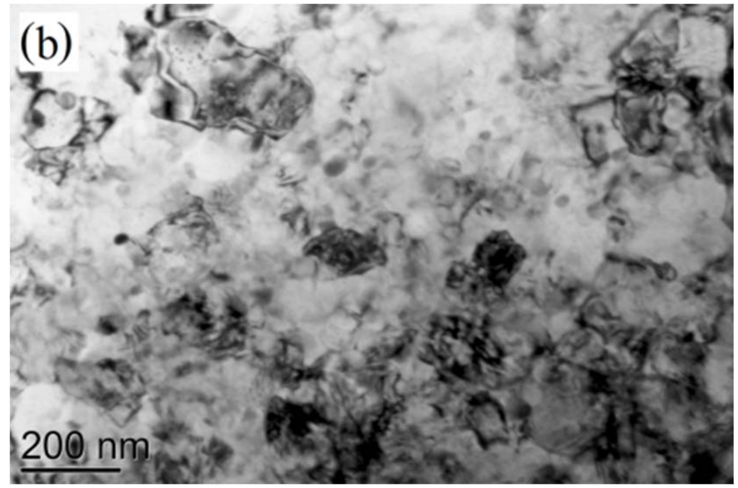

Fe-14Cr-0.5La_2O_3

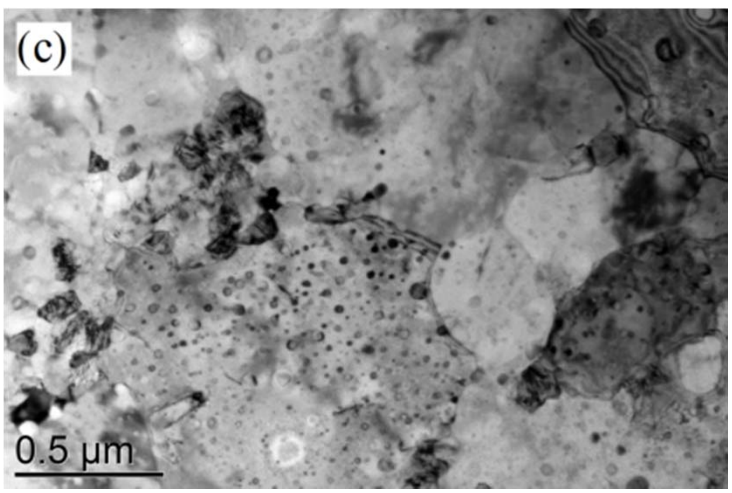

14LMT

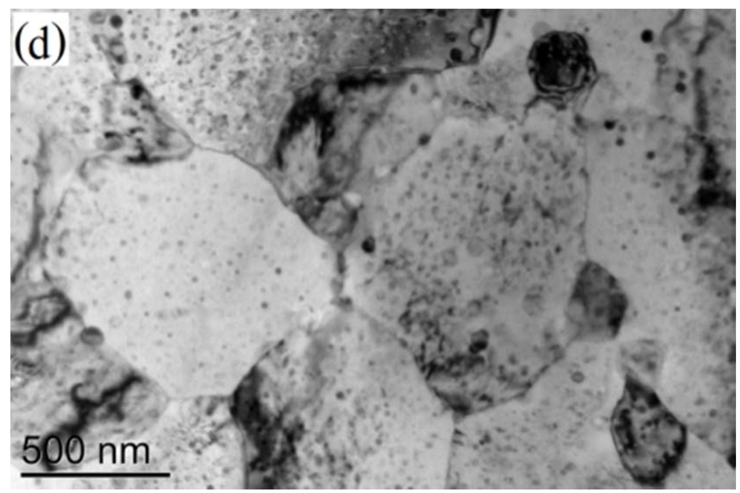

14YMT

Pasebani *et al.*, *J. Alloys & Compounds* 599 (2013) 206

University of Idaho
College of Engineering

Effect of Alloy Composition on Mechanical Properties

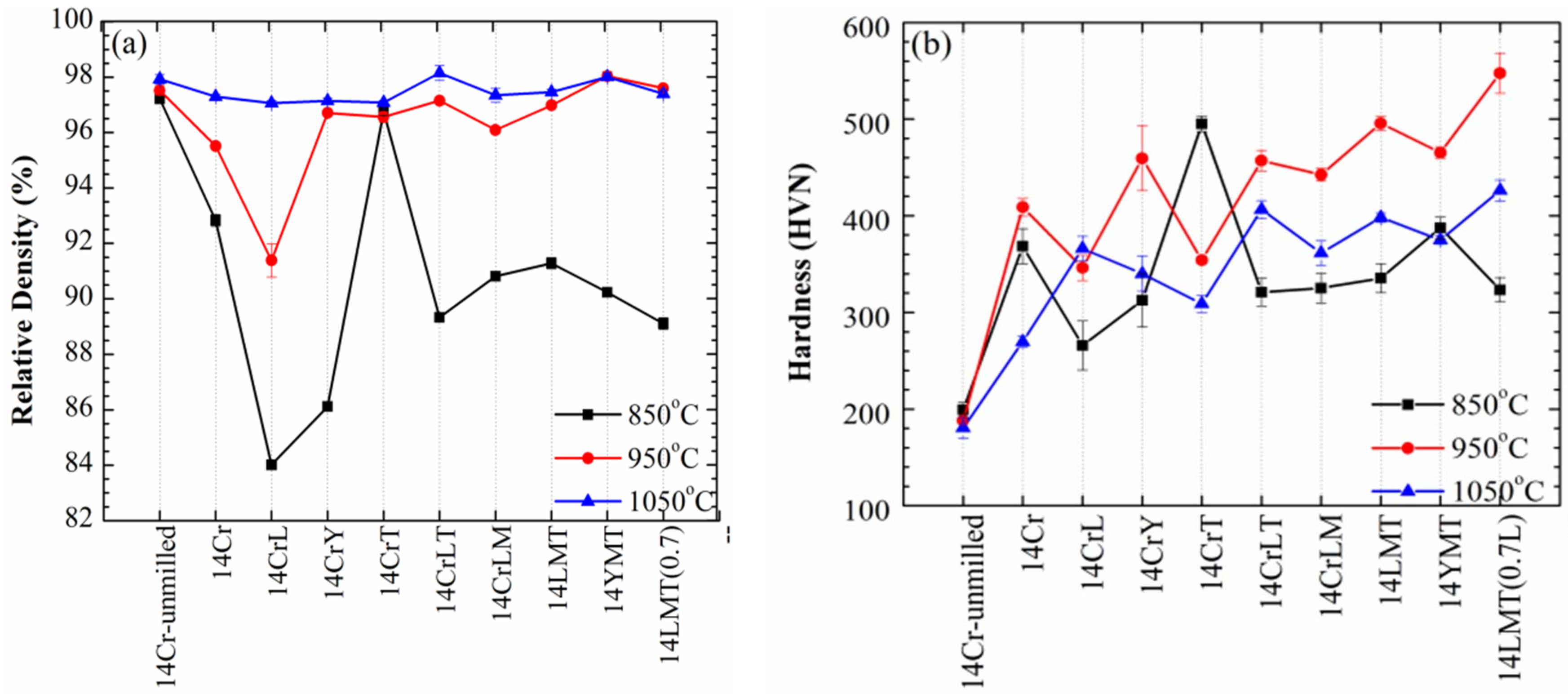

Pasebani *et al., J. Alloys & Compounds* 599 (2013) 206

Effect of Alloy Composition on Oxide Particle Size

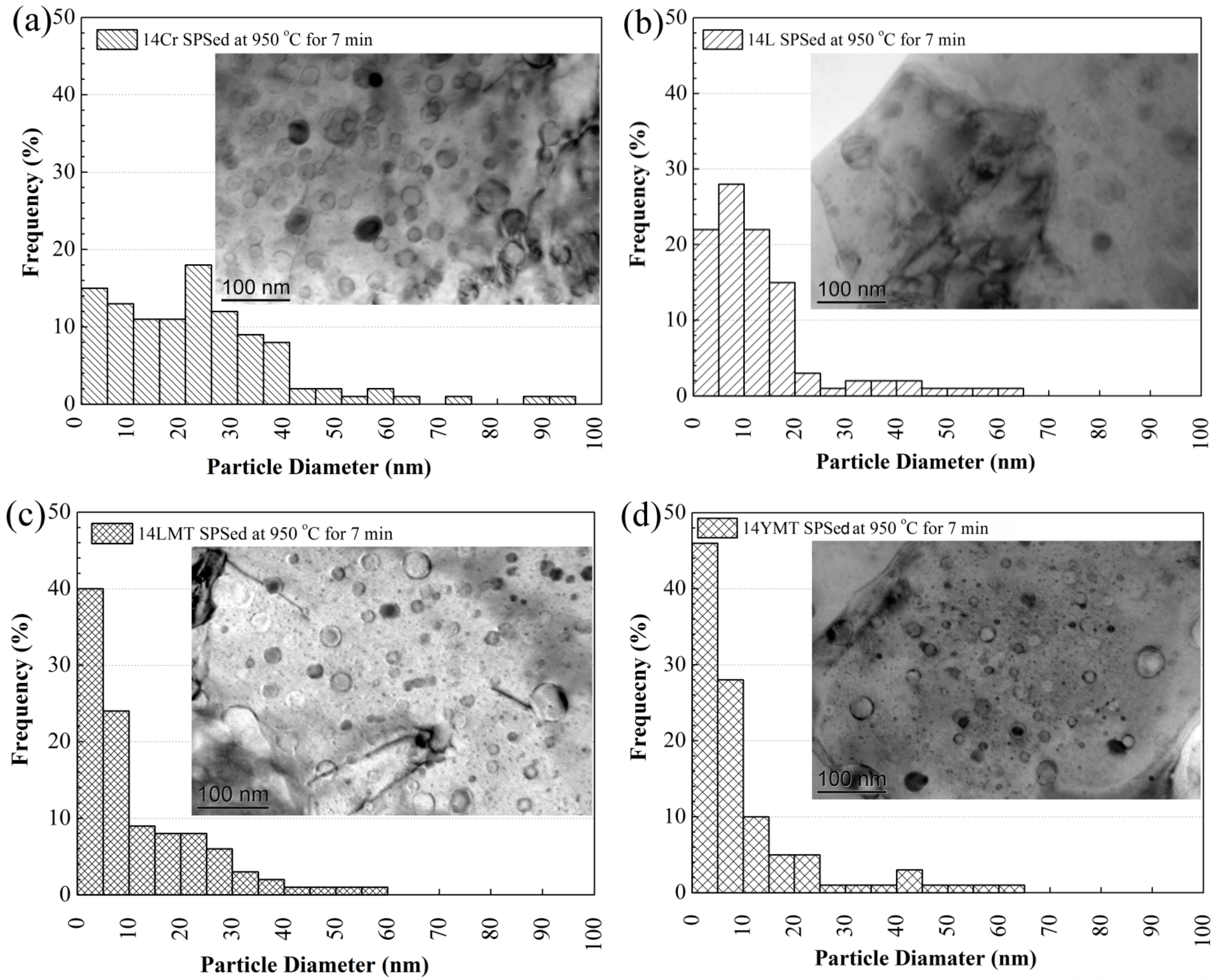

Pasebani *et al.*, 2014

University of Idaho
College of Engineering

Ion Irradiation Experiments

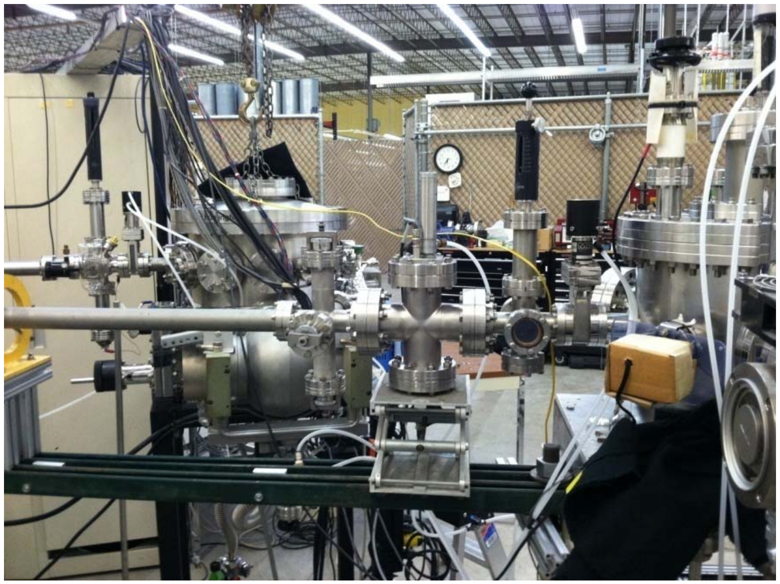

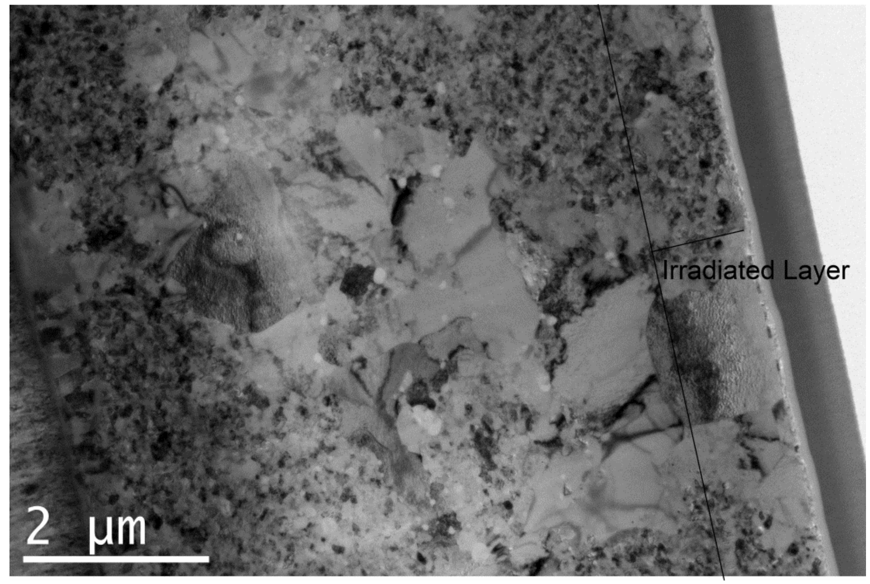

- Texas A&M IMF Lab Accelerator (Dr. Lin Shao)
- Machine: IoneX 1.7 MV Tandetron accelerator
- Ion Source: SNICS sputter source
- At 30 and 500 ^{o}C for 10, 50, and 100 dpa

Microstructure of Irradiated 14LMT

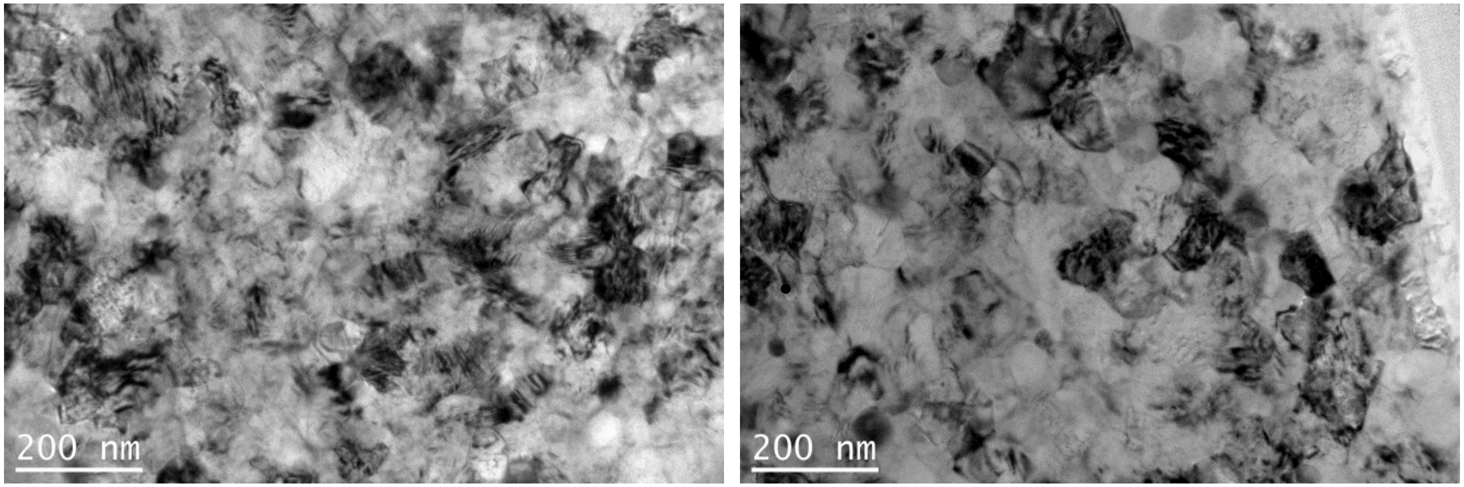

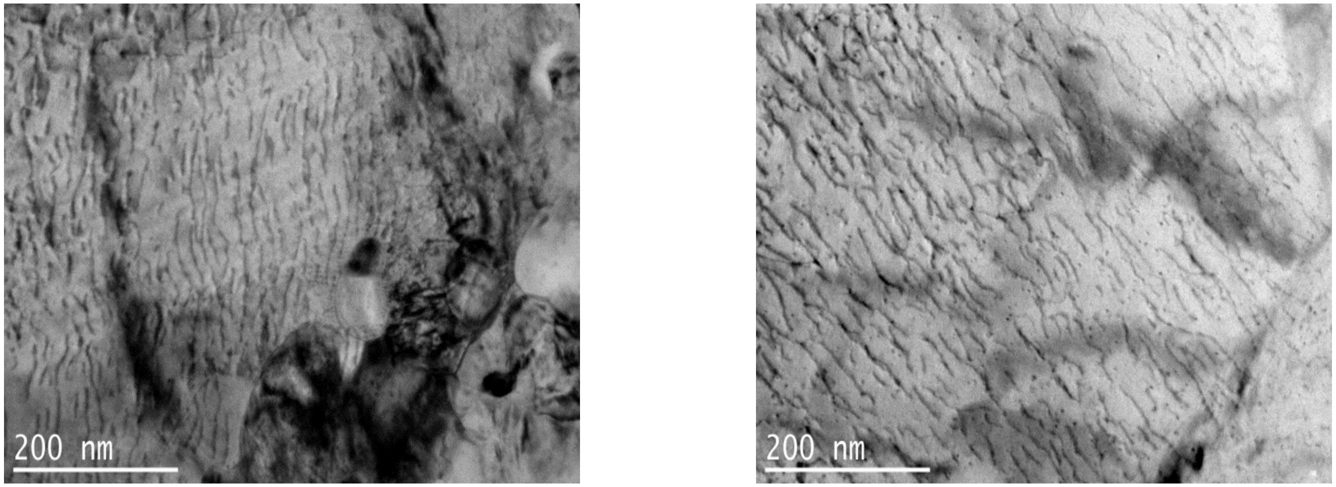

Microstructure and dislocaions:
Un-irradiated

Microstructure and dislocations:
Irradiated 500 ^{o}C for 100 dpa

University of Idaho
College of Engineering

Microstructure of Irradiated 14LMT

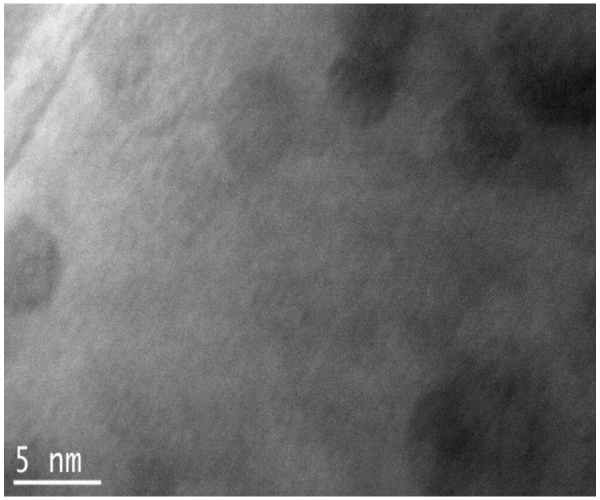

Nanoparticles: Un-irradiated

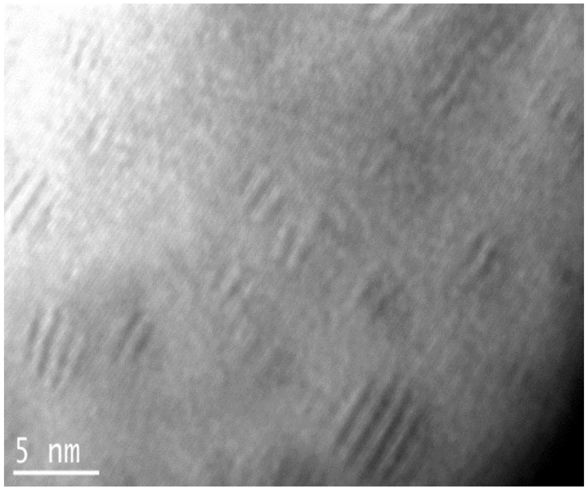

Nanoparticles: Irradiated 500 ºC for 100 dpa

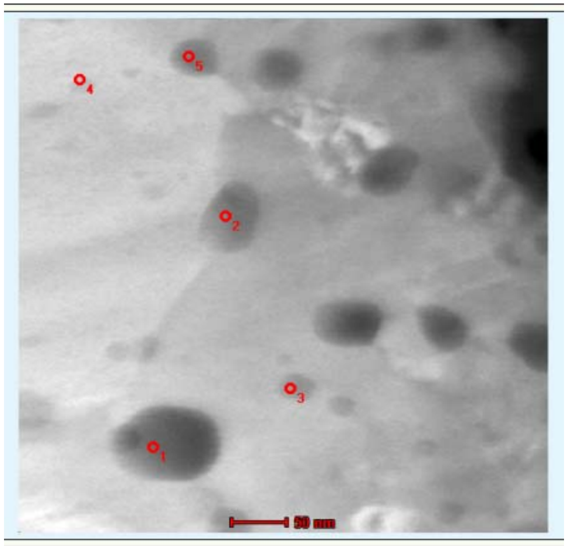

- Nanoparticles size and number density did not show any significant difference after irradiation

STEM HAADF from nanoparticles: Irradiated 500 ºC for 100 dpa

University of Idaho
College of Engineering

Conclusions (I)

- The nucleation of Cr-Ti-La-O nanoclusters during high energy milling was investigated.

- The role of ball milling was more complex than just the dissolution of the solute elements with a significant impact on the densification behavior.

- Adding La and Ti to Fe-14Cr matrix would significantly improve the mechanical behavior and microstructural stability.

Conclusions (II)

- Nano-oxide particles formed before and during the SPS, and hence the interaction of nanoparticles with dislocations and grain boundaries could be complex and impede further recrystallization.

- The APT analysis of the specimen sintered at 950 ^{o}C revealed high number density of 1.2×10^{24} m^{-3} of NCs with the average radius of 1.5 nm, enriched in Cr, Ti, La and O. At 1050 ^{o}C, the number density of NCs decreased to 0.66×10^{24} m^{-3} and the average radius increased slightly.

- High number of NCs along with the Hall-Petch mechanism, dislocation hardening and solid solution hardening led to a significant hardening in the sintered NFSs.

University of Idaho
College of Engineering

Acknowledgments

- This work was supported partly by the Laboratory Directed Research and Development Program of Idaho National Laboratory (INL), Contract DE-AC07-05ID14517, and partly by a grant of the Advanced Test Reactor National Scientific User Facility (ATR NSUF).
- Staff of the Microscopy and Characterization Suite (MaCS) facility at Center of Advanced Energy Studies (CAES).
- Dr. Kun Mo (University of Illinois / Argonne National Laboratory)